Psychiatry Research: Neuroimaging 287 (2019) 49–55

Contents lists available at ScienceDirect

Psychiatry Research: Neuroimaging

journal homepage: www.elsevier.com/locate/psychresns

Dendrite complexity of the posterior cingulate cortex as a substrate for recovery from post-stroke depression: A pilot study

Fumihiko Yasuno[a,b,*], Daisuke Ando[c], Akihide Yamamoto[b], Kazuhiro Koshino[b], Chiaki Yokota[c]

[a] Department of Psychiatry, National Center for Geriatrics and Gerontology, Obu, Japan
[b] Department of Investigative Radiology, National Cerebral and Cardiovascular Center, Suita, Japan
[c] Department of Neurology, National Cerebral and Cardiovascular Center, Suita, Japan

ARTICLE INFO

Keywords:
Post-stroke depression
Resilience
Vulnerability
Diffusion-weighted MRI
GBSS
Neurite orientation dispersion

ABSTRACT

The neural basis of recovery from a depressive state remains poorly understood. The main purpose of this study was to determine the neural basis of vulnerability/resilience to depression in stroke patients in terms of changes in regional microstructure. The study included 20 individuals with acute ischaemic stroke. Symptoms of depression were assessed, and the intraneurite volume fraction and neurite orientation-dispersion index (ODI) were evaluated by a multi-shell diffusion imaging and neurite-orientation dispersion and density imaging model. Patients underwent follow-up examinations after 2 months and were classified into depression improvement and depression deterioration groups. A significant interaction effect of group × time on the ODI was shown by voxel-based analysis in the posterior cingulate cortex (PCC). The ODI change in the PCC was negatively correlated with the change in the depression scale scores at the 2-month time point. The increase in ODI in the PCC that occurred during the 2-month interval was thought to be associated with decreased depressive symptom scores. As the ODI represents the pattern of sprawling dendrite progression, our findings indicate that the dendritic complexity of the PCC is a substrate for recovery in individuals who experienced post-stroke psychosocial and biological stress.

1. Introduction

The differential vulnerability to depression has recently become a topic of interest in psychiatric research (Canli and Lesch, 2007; Hariri and Holmes, 2006). However, the neural basis of vulnerability to depression remains poorly understood. Therefore, there is an urgent need to characterize the neural bases of vulnerability and resilience to depression in order to identify novel targets for therapeutic interventions. Approximately 30–50% of stroke patients experience depression during the first 2 years following stroke (Robinson, 1998), while many patients exhibit resilience to post-stroke depression. Given their high risk of developing depression, the examination of stroke patients might improve our knowledge of the neural mechanisms of resilience and vulnerability to depression.

In recent years, diffusion magnetic resonance imaging (dMRI) has become important for the investigation of the construction of the human brain due to its unique capability to image brain macrostructure and microstructure (Assaf et al., 2013). The diffusion characteristics of water molecules are used in dMRI to assess the cellular microstructural features of brain tissue within the framework of biophysical models. Neurite-orientation dispersion and density imaging (NODDI) has recently been introduced as a multi-component model involving the use of MR diffusion data in which the microstructural complexity of axons and dendrites *in vivo* can be evaluated (Nazeri et al., 2015b). The density and dispersion of neurites are represented by NODDI indices in grey and white matter (GM and WM, respectively) in the brain using the neurite density index (NDI) and orientation dispersion index (ODI), respectively. The organization of dendrites *in vivo* can be evaluated by these indices and provide more insight into the changing cellular architecture than standard indices obtained from diffusion tensor imaging (DTI) (Zhang et al., 2012). The ODI in cortical regions represents the pattern of sprawling dendrite progression and reflects the complexity of GM, while the NDI represents the density of neurites, including axons and dendrites (Song et al., 2008).

NODDI shows tissue alterations associated with normal aging (Billiet et al., 2015; Merluzzi et al., 2016; Nazeri et al., 2015a) and in a range of conditions including focal cortical dysplasia (Winston et al., 2014), stroke (Adluru et al., 2014), Wilson's disease (Song et al., 2018), multiple sclerosis (Grussu et al., 2017), neurofibromatosis type 1 (Billiet et al., 2014; Winston et al., 2014); and neurodegenerative diseases such as Parkinson's disease (Kamagata et al., 2016), Huntington's disease (Zhang et al., 2018), amyotrophic lateral sclerosis (Barritt et al.,

* **Corresponding author at**: Department of Psychiatry, National Center for Geriatrics and Gerontology, 7-430 Morioka-cho, Obu, Aichi 474-8511, Japan.
E-mail address: ejm86rp@yahoo.co.jp (F. Yasuno).

https://doi.org/10.1016/j.pscychresns.2019.01.015
Received 6 November 2018; Received in revised form 4 January 2019; Accepted 21 January 2019
Available online 18 March 2019
0925-4927/

2018), and Alzheimer's disease (Colgan et al., 2016).

The main purpose of this study was to determine the neural basis of resilience/vulnerability to depression in stroke patients based on changes in regional microstructure. NODDI was performed on groups of patients with sub-acute ischaemic stroke. We administered two-month follow-up MRI examinations on patients. All study participants were subjected to quantitative measurements of depressive symptoms on the day of the MRI. Using a voxel-based analysis of NODDI, we compared the characteristics of patients with stroke who exhibited improvement in depressive symptoms with those who exhibited deterioration of depressive symptoms over 2 months.

2. Methods

2.1. Participants

Study participants were recruited and evaluated as previously described (Yasuno et al., 2014). We obtained written informed consent from all participants after providing them with a complete description of the study. This study was approved by the medical ethics committee of the National Cerebral and Cardiovascular Center in Japan and was carried out in accordance with the Declaration of Helsinki. The patients were of Japanese ethnicity and were recruited from the neurology unit of the National Cerebral and Cardiovascular Center hospital. The patients had been initially hospitalized for the treatment of acute ischaemic stroke.

Neurologists diagnosed stroke according to the World Health Organization criteria. After the assessment, the data ware reviewed by a group of psychiatrists and neurologists and a consensus was reached in terms of the presence or absence of psychiatric diseases, including dementia, according to the DSM-IV criteria. Patients were included in the study if they met the following criteria: 1) presence of a focal lesion in either the right or left hemisphere as detected by MRI; 2) absence of other neurological, neurotoxic, or metabolic conditions; 3) modest ischaemic insult (modified Rankin scale score $\leq$ 4) with the absence of a significant verbal comprehension deficit; and 4) occurrence of stroke 14–28 days before the examination. The exclusion criteria were: 1) transient ischaemic attack, cerebral haemorrhage, subdural haematoma, or subarachnoid haemorrhage; 2) history of a central nervous system disease, such as tumour, trauma, hydrocephalus, or Parkinson's disease; and 3) pre-stroke history of depression. Twenty individuals who met the criteria were enrolled in the study. We recruited eleven healthy control participants from the local community via poster advertisements. The exclusion criteria for the healthy participants were a history of or present diagnosis of any mental disorder defined by DSM-5 criteria or neurological illness. Table 1 summarizes the characteristics of this cohort.

We evaluated all stroke patients and control participants using sequential, standardized, quantitative examinations of depressive symptoms and cognitive function on the day of the MRI. Depressive symptoms were assessed using the 15-item Geriatric Depression Scale 15 (GDS), in which a score $\geq$5 indicates depression (Dias et al., 2017; Yesavage et al., 1982). Cognitive impairment was assessed using the Mini-Mental State Examination (MMSE), in which a score $\leq$ 23 indicates cognitive impairment (Folstein et al., 1975).

We used standardized examinations to evaluate the severity of disability/dependence after stroke (modified Rankin scale (mRS); higher scores indicate more severe disability/dependence) (Brott et al., 1989) and stroke severity (National Institutes of Health Stroke Scale (NIHSS); higher scores indicate more severe stroke) (Lyden et al., 2001). All participants underwent MRI examinations. We evaluated the locations, laterality, and the diameter of the infarcts in patients. We classified the seriousness of the white matter hyperintensity (WMH) using the Fazekas scale, which provides a measurement of WMH in the periventricular area (PVH) and deep white-matter (DWMH) (Fazekas et al., 1987).

We administered two-month follow-up MRI examinations on patients. All patients were evaluated by sequential quantitative examinations of depressive symptoms (assessed by the GDS) (Yesavage et al., 1982), cognitive function (assessed by the MMSE) (Folstein et al., 1975), and neurological examination (assessed by the mRS (Brott et al., 1989) and NIHSS (Lyden et al., 2001)) on the day of the follow-up MRI. During the study period, none of the patients with stroke or healthy controls were administered with antidepressant drugs. None of the patients hoped or agreed with the treatment of psychotropic drugs when they were in a depressive mood. Most patients were on antihypertensive, anti-cholesterol, and anticoagulant drugs during the study period.

2.2. Data acquisition using MRI

All MRI examinations were performed using a 3T whole-body scanner (Signa Excite HD V12M4; GE Healthcare, Milwaukee, WI, USA) with an 8-channel phased-array brain coil.

DT images were acquired using a locally modified single-shot echo-planar imaging sequence using parallel acquisition at a reduction (ASSET) factor of two in the axial plane. Whole-brain diffusion-weighted images were collected at two different diffusion-weighted sensitivities: b = 1000 s/mm^2 and b = 2000 s/mm^2 with 29 directions. The b = 1000 s/mm^2 data were used for DTI analysis, while both the b = 1000s/mm^2 and b = 2000s/mm^2 data were used for the NODDI analysis. The echo time (TE) and repetition time (TR) were 71.5 ms and 11,400 ms for the images acquired at b = 1000 s/mm^2, and 83.6 ms and 13,800 ms for images acquired at b = 2000 s/mm^2. Additional brain volumes — for b = 1000 s/mm^2 and b = 2000 s/mm^2 data — were acquired with no diffusion weighting (b = 0 s/mm^2). The other imaging parameters were as follows: acquisition matrix, 128 × 128; field of view (FOV), 256 mm; section thickness, 3.0 mm; no intersection gap; 50 sections. The reconstruction matrix was the same as the acquisition matrix, and 2 × 2 × 3 mm voxel data were obtained. Automated high-order shimming (Kim et al., 2002) was used before conducting the DTI.

High-resolution three-dimensional T1-weighted images were acquired using a fast spoiled gradient-recalled sequence (TR = 12.8 ms; TE = 2.6 ms; inversion time = 600 ms; flip angle = 8°; FOV, 256 mm; 188 sections in the sagittal plane; acquisition matrix, 256 × 256; acquired resolution, 1 × 1 × 1 mm). T2-weighted images were obtained using a fast-spin echo sequence (TR = 4800 ms; TE = 98 ms; echo train length (ETL) = 8; FOV = 256 mm; 50 slices in the transverse plane; acquisition matrix, 160 × 160, acquired resolution, 1.6 × 1.6 × 2 mm).

2.3. Structural MR imaging analysis

Image pre-processing and statistical analysis were performed as previously described (Morimoto et al., 2018) using Statistical Parametric Mapping software (SPM12, Wellcome Trust Centre for Neuroimaging, London, UK; http://www.fil.ion.ucl.ac.uk/spm). Voxel-based morphometry was conducted using the Computational Anatomy Toolbox for SPM (CAT12; Jena University Hospital Departments of Psychiatry and Neurology, Jena, Germany; http://dbm.neuro.uni-jena.de/cat/) in a MATLAB R2017a environment (MathWorks, Natick, MA). The default pre-processing approach was used to analyse the longitudinal data in CAT12. T1-weighted images were subjected to intra-subject realignment; bias correction; tissue segmentation into GM, white matter (WM), and cerebrospinal fluid; and registration using linear (affine registration) and nonlinear transformations via Diffeomorphic Anatomical Registration Through Exponentiated Lie Algebra (Ashburner and Friston, 2005) within a unified model (Ashburner, 2007). We subsequently analysed GM and WM segments by multiplying them by the nonlinear components derived from the normalization matrix for the preservation of actual local GM and WM values (modulated GM and WM volumes).

Table 1
Demographic characteristics of the patients and healthy control subjects.

Characteristic	Patients exhibiting depression improvement (n = 11)	Patients exhibiting depression deterioration (n = 9)	t_{18} or χ_1^{2a}	P	Healthy controls (n = 11)	$F_{2,28}$ or $\chi^2{}_2{}^b$	P
Age (years)	63.7 ± 5.5	61.0 ± 8.8	t = 0.85	0.41	66.9 ± 1.0	F = 2.62	0.09
Female sex (n,%)	1 (9.1)	3 (33.3)	χ^2 = 1.82	0.18	5 (45.5)	χ^2 = 3.64	0.16
Education (years)	14.1 ± 2.8	13.1 ± 2.3	t = 0.85	0.41	13.1 ± 2.3	F = 0.46	0.64
MMSE score	28.8 ± 1.4	28.3 ± 2.6	t = 0.54	0.60	28.3 ± 1.5	F = 0.20	0.82
1st examination							
2nd examination	29.0 ± 1.0	28.4 ± 2.7	t = 0.64	0.53		F = 0.35	0.71
GDS score	7.0 ± 4.2	4.2 ± 2.8	t = 1.68	0.11	1.9 ± 1.9	F = 6.88	0.004**
1st examination							
2nd examination	4.9 ± 3.9	6.3 ± 3.0	t = 0.91	0.38		F = 5.51	0.01**
mRS score	0.9 ± 0.7	0.8 ± 0.6	t = 0.07	0.95			
1st examination							
2nd examination	0.8 ± 0.9	0.9 ± 0.6	t = 0.21	0.84			
NIHSS score	0.9 ± 0.7	0.8 ± 1.1	t = 0.33	0.75			
1st examination							
2nd examination	0.4 ± 0.5	0.6 ± 0.7	t = 0.70	0.50			
Acute infarcts (n,%) in:							
Basal ganglia	3 (27.2)	1(11.1)	χ^2 = 0.81	0.37			
Subcortical white matter	5 (45.5)	4 (44.4)	χ^2 = 0.002	0.96			
Thalamus	3 (27.2)	4 (44.4)	χ^2 = 0.64	0.42			
Laterality of acute hemisphere infarcts							
Left hemisphere (n,%)	5 (45.5)	3 (33.3)	χ^2 = 0.30	0.58			
The diameter of infarcts (mm)	9.6 ± 3.7	10.1 ± 4.5	t = 0.26	0.80			
Fazekas DWMH score (n,%)							
0–2	9 (81.8)	6 (66.7)					
3	2 (18.2)	3 (33.3)	χ^2 = 0.61	0.44			
Fazekas PVH score (n,%)							
0–2	10 (90.9)	8 (88.9)					
3	1 (9.1)	1 (11.1)	χ^2 = 0.02	0.88			

Data are presented as mean ± sd. *$p < 0.05$.
** $p < 0.01$.
[a] The differences in the two patient groups were examined using t- or χ^2- tests.
[b] The differences among groups of patients and healthy controls were examined using ANOVA or χ^2- tests
Abbreviations: MMSE, Mini-Mental State Examination; GDS, geriatric depression scale; mRS, modified Rankin scale; NIHSS, National Institutes of Health Stroke Scale; DWMH, deep white-matter hyperintensity; PVH paraventricular area white matter hyperintensity.

2.4. Pre-processing of diffusion MR imaging

We performed the pre-processing of diffusion MR imaging as previously described by Chang et al. (2015). We used FMRIB's Linear Image Registration Tool (FLIRT; www.fmrib.ox.ac.uk/fsl/flirt) to register all diffusion-weighted volumes to their corresponding $b = 0$ s/mm^2 volume, and to correct for motion and eddy currents (Jenkinson et al., 2002). We estimated the relative displacements between consecutive diffusion volumes for each subject, and no participants exhibited >2-mm average displacement; therefore, no patients were excluded due to excessive motion. Afterward, we used the Brain Extraction Tool (http://www.fmrib.ox.ac.uk/analysis/research/bet) to eliminate non-brain tissue, and FSL's DTIFIT was used to calculate maps of fractional anisotropy (FA) and mean diffusivity (MD) (Chang et al., 2015).

We fitted the NODDI model using the NODDI toolbox (https://www.nitrc.org/projects/noddi_toolbox/) in the MATLAB environment (Zhang et al., 2012). A complementary model of diffusion using NODDI was allowed by the acquisition of diffusion data using two different diffusion weightings ($b = 1000$ s/mm^2 and $b = 2000$ s/mm^2). We normalized data by $b = 0$ volumes to account for the differing TE/TR times between lower and higher shells. Maps of NDI and ODI were created using this modelling paradigm for each subject (Chang et al., 2015).

2.5. Diffusion metric voxel-wise analysis

We used FSL's Tract-Based Spatial Statistics (TBSS) tool (Smith et al., 2006) for aligning individual FA maps to FSL's standard adult FA template. After registration, we thinned the FA maps of all participants to create WM skeletons. Next, we created and registered MD, ODI, and NDI maps in the WM by using the TBSS registrations of FA to the adult FA template, and we applied the skeleton mask to the registered images (Chang et al., 2015).

GM-based spatial statistics (GBSS) methodology (Ball et al., 2013; Nazeri et al., 2015b) was adopted to examine ODI and NDI in GM in a voxel-wise fashion (NODDI-GBSS; https://github.com/arash-n/GBSS/blob/master/README.md). This method is a GM analogue of TBSS (Smith et al., 2006) and ensures accurate anatomical alignment between participants with the use of a skeleton projection step. By creating a skeleton map of the cerebral cortex and consolidating the parameters of the surrounding regions into those of the skeleton, it is possible to avoid partial volume effects of WM and cerebrospinal fluid. Voxel-based analysis using SPM12 was performed on TBSS- and GBSS-derived skeletonized parameter maps

2.6. Statistical analysis

The interaction effect of group (patients with depression improvement versus deterioration) × time (subacute stage versus 2 months follow-up) on the volumes, FA, MD, NDI, and ODI in the longitudinal analysis was examined by flexible factorial design which can be done by voxel-based analysis using SPM12. In this analysis, we smoothed the normalized parameter maps using a Gaussian kernel of 8-mm full-width at half-maximum. In this voxel-based analysis, we applied a height threshold of uncorrected $p < 0.001$ with a cluster-extent threshold of $p < 0.05$ (uncorrected).

We assessed the VOIs from clusters in which significant interactions were found. The same VOIs were set in the control groups, and we calculated regional values by averaging the values for all voxels within

the VOIs in the patient and control groups. We compared the VOI value changes over the 2 months of follow-up between the two patient groups using a paired *t*-test. Pearson's correlation analysis was used to examine how VOI value changes were related to the changes in the depression scale scores over the 2 months of follow-up. VOI values were compared between patients and controls groups using a *t*-test. Statistical analyses were performed using SPSS for Windows 22.0 (IBM Japan Inc., Tokyo, Japan).

3. Results

3.1. Demographic and clinical data

Table 1 showed the study participants' demographic and clinical characteristics. According to their change in depression scale score over 2 months, the stroke patients were classified into either the depression improvement group (DI group; change in score <0; $n = 11$) or the depression deterioration group (DD group; change in score ≥ 0; $n = 9$). There was no significant difference between the two patient groups and among patient and healthy control groups with regard to age, sex, or education level.

There was no significant difference between the two patient groups, and between patient and healthy controls with regard to MMSE scores. In addition, no significant group differences were observed in patients with regard to GDS scores. We found significantly higher GDS scores in both patient groups when compared with healthy control participants. Eleven of 20 patient with stroke showed depression (GDS score ≥ 5), while none of the control participants showed depression during the study period.

Repeated measures analysis of variance (ANOVA) indicated no significant effect of time (subacute stage versus 2 months follow-up; $F_{1, 18} = 0.34$, $p = 0.57$) or interaction between group and time ($F_{1, 18} = 0.02$, $p = 0.89$) on the MMSE score, while there was a significant interaction between group and time ($F_{1, 18} = 37.6$, $p < 0.001$) on the GDS score.

We found no significant differences in the mRS/NIHSS scores between groups. Repeated measures ANOVA indicated a significant effect of time on the NIHSS score ($F_{1, 18} = 14.6$, $p = 0.001$ for the NIHSS score, $F_{1, 18} = 0.47$, $p = 0.50$ for the mRS score). We found no significant interaction between group and time on the NIHSS ($F_{1, 18} = 0.85$, $p = 0.37$) or mRS scores ($F_{1, 18} = 0.005$, $p = 0.95$). The two patient groups exhibited no significant difference in the location, laterality of hemisphere, or diameter of infarcts. There were no significant group differences in the ratio of patients with Fazekas scores >3.

3.2. Voxel-based analysis of interaction effect of group × time

Voxel-based analysis revealed a significant interaction effect of group × time on the ODI in the posterior cingulate cortex (PCC) in GM of the stroke patients ([*x, y, z*] = [–8, –32, 40], cluster voxel size = 65, $T = 5.70$; height threshold of uncorrected $p < 0.001$ with cluster-extent threshold of $p < 0.05$; Fig. 1). No patients had lesions in the PCC. We found no other significant interaction effects of volume, ODI, NDI, FA, and MD in GM or WM of the stroke patients.

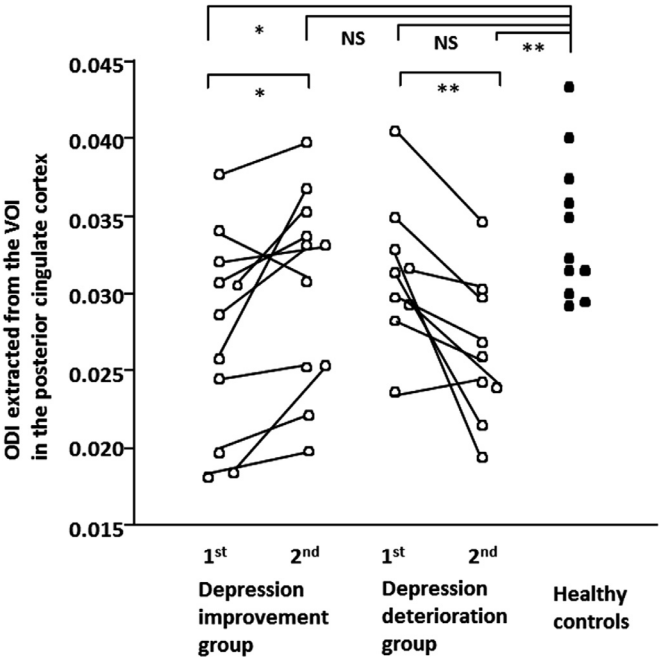

Fig. 2. Scatterplots illustrating the ODI values in the posterior cingulate cortex in patients and controls
We found a significant increase in the ODI in patients in the depression improvement group and a significant decrease in the ODI in patients in the depression deterioration group. There was a significant decrease in the posterior cingulate cortex-ODI in the patients in the depression improvement group at the 1st examination and in patients in the depression deterioration group at the 2nd examination compared with healthy controls.
ODI: orientation-dispersion index, VOI: volumes of interest
NS: not significant, $^*p < 0.05$, $^{**}p < 0.01$.

We found a significant interaction effect of group × time on the ODI value in the PCC with repeated measures ANOVA ($F_{1,18} = 20.9$, $p < 0.001$).

It was reported that the microstructural alterations elucidated by NODDI are sensitive to age and sex (Kodiweera et al., 2016). Further, laterality of infarction, diameter of infarcts, DWMH, and NIHSS score, and the existence of depression at 1st examination could be regarded as the potential confounding factor of the stroke patients. However, after adjusting for the confounding effects of age, sex, laterality of infarction, diameter of infarcts, DWMH, NIHSS score, and the existence of depression at 1st examination (GDS score ≥ 5; $n = 11$), the interaction remained significant ($F_{1,11} = 24.6$, $p < 0.001$). We found a significant increase in the ODI value in patients in the DI group ($t_{10} = 2.87$, $p = 0.017$; 0.027 ± 0.007 at the first examination, 0.030 ± 0.006 at the second examination) and a significant decrease in the ODI value in patients in the DD group ($t_8 = 3.44$, $p = 0.009$; 0.031 ± 0.005 at the first examination, 0.026 ± 0.005 at the second examination) as determined by a paired *t*-test (Fig. 2).

The PCC-ODI values in the DI group patients at the first examination

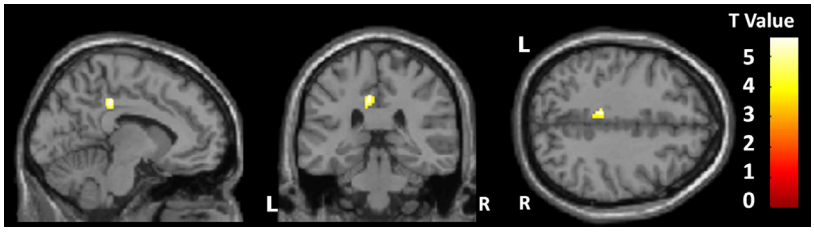

Fig. 1. Voxel-based analysis revealed a significant interaction effect of group × time on the orientation-dispersion index in the posterior cingulate cortex of patients
Images are presented in radiological orientation. Detected areas exceeded an uncorrected $p < 0.001$ with cluster-extent threshold of $p < 0.05$. Adjustments for multiple testing were not performed at cluster level. These statistical parametric mapping projections were then superimposed on representative sagittal ($x = -8$), coronal ($y = -32$), and transaxial ($z = 40$) magnetic resonance images.
L: left, R: right.

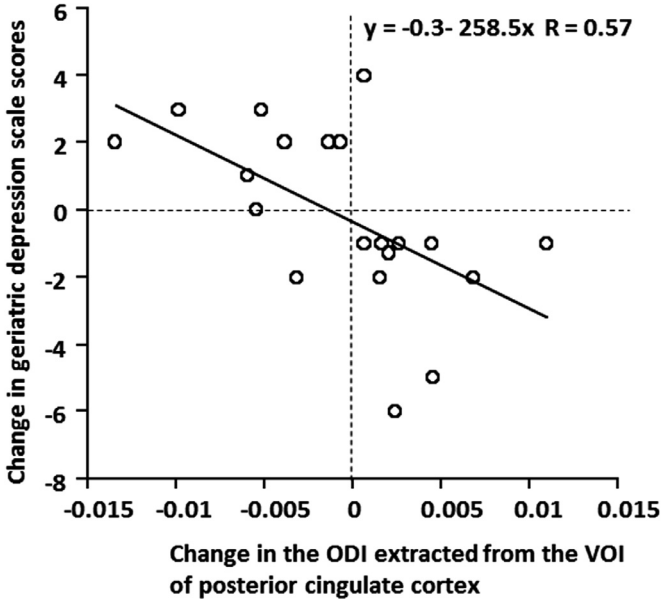

Fig. 3. Scatterplots illustrating the relationship between the changes in ODI in the posterior cingulate cortex and the depression scale scores over 2 months in stroke patients

A significant negative correlation was observed between the ODI change and the depression scale score (r = –0.57, p = 0.009). The correlation in patients remained significant after partial correlation analysis with age, sex, education, laterality of the infarction, and NIHSS score (r = –0.70, p = 0.005).

ODI, orientation-dispersion index; VOI: volumes of interest; NIHSS, National Institutes of Health Stroke Scale.

(t_{20} = 2.82, p = 0.01) and those in the DD group patients at the second examination (t_{18} = 3.76, p = 0.001) were significantly lower than those in the healthy controls (0.034 ± 0.005), as determined by an unpaired t-test. After adjusting for the confounding effects of age and sex with ANCOVA, the difference remained significance ($F_{1,18}$ = 6.7, p = 0.02 for the DI group at the first examination, $F_{1,16}$ = 9.1, p = 0.008 for the DD group at the second examination)

In the analysis of the relationship between the change in PCC-ODI and the depression scale scores, there was a significant negative relationship between the change in the depression scale scores and the change in the ODI in VOIs in the PCC over 2 months in the stroke patients (r = −0.57, p = 0.009) (Fig. 3). After accounting for the confounding effects of age, sex, laterality of infarction, diameter of infarcts, DWMH, NIHSS score, and the existence of depression at 1st examination as covariates in a partial correlation analysis, the negative relationship remained significant (r = –0.68, p = 0.02). A multiple regression analysis was used to evaluate whether the change in the PCC-ODI was related to the change in the depression scale scores using the covariates of age, sex, laterality of infarction, diameter of infarcts, DWMH, NIHSS score, and the existence of depression at 1st examination and found that the change in ODI values negatively correlated with the change in the depression scale scores (beta = –0.58, p = 0.02).

4. Discussion

Our findings indicate that patients with stroke who exhibited improvements in the depression scale scores also exhibited significantly greater ODI increases in the PCC than did those who exhibited depression scale score deterioration over the 2 months following the subacute stage of ischaemic stroke. Furthermore, the ODI change in the PCC was negatively correlated with the score change in the depression scale over a 2-month interval. The increased ODI in the PCC during the 2-month interval was associated with decreased depression scale scores. The ODI in cortical regions is representative of the pattern of sprawling dendrite progression and can reflect the complexity of GM (Song et al., 2008). Our results, which showed an association between the PCC-ODI increase and the recovery from a depressive state, indicate that the sprawling dendrite progression in the PCC may be a substrate for recovery in individuals who experience post-stroke psychosocial and biological stress.

Lesion location has been extensively investigated as a risk factor for PSD. Patients with acute stroke with left frontal or left basal ganglia lesions had a significantly higher frequency of depression (Robinson et al., 1984; Starkstein et al., 1987). However, a subsequent meta-analysis of the data from patients with stroke reported no significant association between depression and lesion location (Ayerbe et al., 2013; Kutlubaev and Hackett, 2014). Robinson and Jorge (2016) indicated that the lack of association was considered to be due to a heterogeneity of assessment methods for depression in this studies, the diverse timing of the assessments, different definitions of lesion location, and different neuroimaging methods used to determine lesion location.

The importance of the role of the PCC has been indicated by a number of studies in emotion-related cognitive processes, including the evaluation of emotion (Wright et al., 2008), processing of happy and sad words (Maddock et al., 2003), and social behaviour (Adolphs, 2003). Individuals with greater PCC activity have been shown to be able to resolve moods of depression more easily (Mayberg et al., 2005). Functional MRI in healthy individuals and those with mood disorders showed that negative functional coupling was observed between the activity of the PCC and the amygdala, an important brain structure for the processing and regulation of emotion (McClure et al., 2007). The importance of the PCC was supported by findings showing that the amygdala modulates activity during mood regulation (Fang et al., 2013). Our findings indicated that the sprawling dendrite progression of the PCC might have association with the modulation of emotion-related cognitive processes in the amygdala during the control of mood. This modulation could then elicit improvement in post-stroke depressive symptoms.

Clinical studies of patients who have “recovered” from stroke have demonstrated an increasing amount of evidence that functional reorganization occurs within the homotopic intact cortex (Cramer et al., 1997; Cuadrado et al., 1999; Kopp et al., 1999). Electrolytic lesioning in the sensorimotor cortex in rats demonstrated that an increase in dendritic complexity was triggered within the opposite, undamaged sensorimotor cortex (Jones and Schallert, 1992 1994). The ODI in cortical regions represents the complexity of GM (Song et al., 2008), and our *in vivo* results agree with previous animal studies on the dendritic change in intact regions after brain damage. Our findings of PCC-ODI increase in patients who recovered from a depressive state may represent an increase of dendritic complexity due to the sprawling dendrite progression triggered within the intact PCC after stroke. The difference in dendritic complexity changes in the PCC may relate to individual differences predicting whether post-stroke stressors will lead to depression or resilience.

The study has several limitations. First, the sample size of this pilot study is modest (20 patients, each scanned twice), though the within-subject study design partially buffered this shortcoming by improving statistical power and sensitivity. The results should be verified by future studies conducted on larger cohorts. Second, the stroke patients' ischaemic insults in our study were modest. Therefore, the effect of the severity of the insult on our findings is uncertain. Third, important variables for the recovery from depression, such as social support and pre-morbid personality, were not controlled. Finally, there has been some criticism of the NODDI model in terms of its many assumptions, which could cause either a negative or positive bias in the NODDI indices (Jelescu et al., 2016; Lampinen et al., 2017). However, as indicated by Dowell et al. (2018), all models that use the microstructure from diffusion-weighted imaging data have some assumptions, and improved characterization of the tissue microstructure was provided by NODDI in comparison with simplistic models such as DTI.

In summary, patients with stroke who exhibited improvement in depressive symptoms also exhibited significantly greater ODI increases in the PCC than patients who exhibited depressive deterioration over the 2-month period following a subacute stage of ischaemic stroke. Furthermore, the ODI change in the PCC was negatively correlated with the score changes in the depression scale over the 2 months. These results indicated that the sprawling dendrite progression shown as the ODI change in the PCC was a substrate for recovery from post-stroke depression. Our findings highlight the importance of a comprehensive understanding of the role and therapeutic potential of dendritic change in the PCC in individuals who have experienced post-stroke psychosocial and biological stress.

CRediT authorship contribution statement

Fumihiko Yasuno: Writing - original draft, Formal analysis, Writing - review & editing, Data curation, Visualization. **Daisuke Ando:** Writing - review & editing, Formal analysis, Data curation, Visualization. **Akihide Yamamoto:** Formal analysis, Writing - review & editing. **Kazuhiro Koshino:** Writing - review & editing, Data curation. **Chiaki Yokota:** Writing - review & editing, Data curation, Visualization, Data curation.

Acknowledgements

We would like to thank the members of the MRI facility staff of the Department of Investigative Radiology at the National Cerebral and Cardiovascular Center in Japan for carrying out the acquisition of MRI data and caring for all participants during the MRI procedures.

Funding

This research was supported by Grants-in-Aid for Scientific Research (C) 15K09841 and 16K10747 from the Japan Society for the Promotion of Science.

Conflict of interest

The authors have no conflicts of interest to disclose. The sponsor had a role in neither the analysis nor interpretation of these data nor in the content of the paper. Appropriate approval procedures were used concerning participants.

Supplementary materials

Supplementary material associated with this article can be found, in the online version, at doi:10.1016/j.pscychresns.2019.01.015.

References

Adluru, G., Gur, Y., Anderson, J.S., Richards, L.G., Adluru, N., DiBella, E.V., 2014. Assessment of white matter microstructure in stroke patients using NODDI. In: Conf Proc IEEE Eng Med Biol Soc. 2014. pp. 742–745.
Adolphs, R., 2003. Cognitive neuroscience of human social behaviour. Nat. Rev. Neurosci. 4, 165–178.
Ashburner, J., 2007. A fast diffeomorphic image registration algorithm. Neuroimage 38, 95–113.
Ashburner, J., Friston, K.J., 2005. Unified segmentation. Neuroimage 26, 839–851.
Assaf, Y., Alexander, D.C., Jones, D.K., Bizzi, A., Behrens, T.E., 2013. The CONNECT project: combining macro-and micro-structure. Neuroimage 80, 273–282.
Ayerbe, L., Ayis, S., Wolfe, C.D., Rudd, A.G., 2013. Natural history, predictors and outcomes of depression after stroke: systematic review and meta-analysis. Br. J. Psychiatry 202, 14–21.
Ball, G., Srinivasan, L., Aljabar, P., Counsell, S.J., Durighel, G., Hajnal, J.V., et al., 2013. Development of cortical microstructure in the preterm human brain. Proc. Natl. Acad. Sci. U S A 110, 9541–9546.
Barritt, A.W., Gabel, M.C., Cercignani, M., Leigh, P.N., 2018. Emerging Magnetic Resonance Imaging Techniques and Analysis Methods in Amyotrophic Lateral Sclerosis. Front. Neurol. 9, 1065.
Billiet, T., Madler, B., D'Arco, F., Peeters, R., Deprez, S., Plasschaert, E., et al., 2014. Characterizing the microstructural basis of "unidentified bright objects" in neurofibromatosis type 1: a combined in vivo multicomponent T2 relaxation and multi-shell diffusion MRI analysis. Neuroimage Clin. 4, 649–658.
Billiet, T., Vandenbulcke, M., Madler, B., Peeters, R., Dhollander, T., Zhang, H., et al., 2015. Age-related microstructural differences quantified using myelin water imaging and advanced diffusion MRI. Neurobiol. Aging 36, 2107–2121.
Brott, T., Adams, H.P.J., Olinger, C.P., Marler, J.R., Barsan, W.G., Biller, J., et al., 1989. Measurements of acute cerebral infarction: a clinical examination scale. Stroke 20, 864–870.
Canli, T., Lesch, K.P., 2007. Long story short: the serotonin transporter in emotion regulation and social cognition. Nat. Neurosci. 10, 1103–1109.
Chang, Y.S., Owen, J.P., Pojman, N.J., Thieu, T., Bukshpun, P., Wakahiro, M.L., et al., 2015. White matter changes of neurite density and fiber orientation dispersion during human brain maturation. PloS one 10, e0123656.
Colgan, N., Siow, B., O'Callaghan, J.M., Harrison, I.F., Wells, J.A., Holmes, H.E., et al., 2016. Application of neurite orientation dispersion and density imaging (NODDI) to a tau pathology model of Alzheimer's disease. Neuroimage 125, 739–744.
Cramer, S.C., Nelles, G., Benson, R.R., Kaplan, J.D., Parker, R.A., Kwong, K.K., et al., 1997. A functional MRI study of participants recovered from hemiparetic stroke. Stroke 28, 2518–2527.
Cuadrado, M.L., Egido, J.A., Gonzalez-Gutierrez, J.L., Varela-De-Seijas, E., 1999. Bihemispheric contribution to motor recovery after stroke: a longitudinal study with transcranial doppler ultrasonography. Cerebrovasc. Dis. 9, 337–344.
Dias, F., Teixeira, A.L., Guimaraes, H.C., Barbosa, M.T., Resende, E.P.F., Beato, R.G., et al., 2017. Accuracy of the 15-item Geriatric Depression Scale (GDS-15) in a community-dwelling oldest-old sample: the Pieta Study. Trends Psychiatry Psychother. 39, 276–279.
Dowell, N.G., Bouyagoub, B., Tibble, J., Voon, V., Cetcingnani, M., Harrison, N.A., 2018. Interferon-alpha-Induced changes in NODDI predispose to the development of fatigue. Neruroscience in press.
Fang, Z., Zhu, S., Gillihan, S.J., Korczykowski, M., Detre, J.A., Rao, H., 2013. Serotonin transporter genotype modulates functional connectivity between amygdala and PCC/PCu during mood recovery. Front. Hum. Neurosci. 7, 704.
Fazekas, F., Chawluk, J.B., Alavi, A., Hurtig, H.I., Zimmerman, R.A., 1987. MR signal abnormalities at 1.5 T in Alzheimer's dementia and normal aging. AJR Am. J. Roentgenol. 149, 351–356.
Folstein, M.F., Folstein, S.E., McHugh, P.R., 1975. "Mini-mental state". A practical method for grading the cognitive state of patients for the clinician. J. Psychiatr. Res. 12, 189–198.
Grussu, F., Schneider, T., Tur, C., Yates, R.L., Tachrount, M., Ianus, A., et al., 2017. Neurite dispersion: a new marker of multiple sclerosis spinal cord pathology? Ann. Clin. Transl. Neurol. 4, 663–679.
Hariri, A.R., Holmes, A., 2006. Genetics of emotional regulation: the role of the serotonin transporter in neural function. Trends Cogn. Sci. 10, 182–191.
Jelescu, I.O., Veraart, J., Fieremans, E., Novikov, D.S., 2016. Degeneracy in model parameter estimation for multi-compartmental diffusion in neuronal tissue. NMR Biomed. 29, 33–47.
Jenkinson, M., Bannister, P., Brady, M., Smith, S., 2002. Improved optimization for the robust and accurate linear registration and motion correction of brain images. Neuroimage 17, 825–841.
Jones, T.A., Schallert, T., 1992. Overgrowth and pruning of dendrites in adult rats recovering from neocortical damage. Brain Res. 581, 156–160.
Jones, T.A., Schallert, T., 1994. Use-dependent growth of pyramidal neurons after neocortical damage. J. Neurosci. 14, 2140–2152.
Kamagata, K., Hatano, T., Okuzumi, A., Motoi, Y., Abe, O., Shimoji, K., et al., 2016. Neurite orientation dispersion and density imaging in the substantia nigra in idiopathic Parkinson disease. Eur. Radiol. 26, 2567–2577.
Kim, D.H., Adalsteinsson, E., Glover, G.H., Spielman, D.M., 2002. Regularized higher-order in vivo shimming. Magn. Reson. Med. 48, 715–722.
Kodiweera, C., Alexander, A.L., Harezlak, J., McAllister, T.W., Wu, Y.C., 2016. Age effects and sex differences in human brain white matter of young to middle-aged adults: a DTI, NODDI, and q-space study. Neuroimage 128, 180–192.
Kopp, B., Kunkel, A., Muhlnickel, W., Villringer, K., Taub, E., Flor, H., 1999. Plasticity in the motor system related to therapy-induced improvement of movement after stroke. Neuroreport 10, 807–810.
Kutlubaev, M.A., Hackett, M.L., 2014. Part II: predictors of depression after stroke and impact of depression on stroke outcome: an updated systematic review of observational studies. Int. J. Stroke 9, 1026–1036.
Lampinen, B., Szczepankiewicz, F., Martensson, J., van Westen, D., Sundgren, P., Nilsson, M., 2017. Neurite density imaging versus imaging of microscopic anisotropy in diffusion MRI: a model comparison using spherical tensor encoding. Neuroimage 147, 517–553.
Lyden, P.D., Lu, M., Levine, S.R., Brott, T.G., Broderick, J., NINDS rtPA Stroke Study Group., 2001. A modified National Institutes of Health Stroke Scale for use in stroke clinical trials: preliminary reliability and validity. Stroke 32, 1310–1317.
Maddock, R.J., Garrett, A.S., Buonocore, M.H., 2003. Posterior cingulate cortex activation by emotional words: fMRI evidence from a valence decision task. Hum. Brain. Mapp. 18, 30–41.
Mayberg, H.S., Lozano, A.M., Voon, V., McNeely, H.E., Seminowicz, D., Hamani, C., et al., 2005. Deep brain stimulation for treatment-resistant depression. Neuron 45, 651–660.
McClure, E.B., Monk, C.S., Nelson, E.E., Parrish, J.M., Adler, A., Blair, R.J., et al., 2007. Abnormal attention modulation of fear circuit function in pediatric generalized anxiety disorder. Arch. Gen. Psychiatry 64, 97–106.
Merluzzi, A.P., Dean 3rd, D.C., Adluru, N., Suryawanshi, G.S., Okonkwo, O.C., Oh, J.M., et al., 2016. Age-dependent differences in brain tissue microstructure assessed with

neurite orientation dispersion and density imaging. Neurobiol. Aging 43, 79–88.
Morimoto, T., Matsuda, Y., Matsuoka, K., Yasuno, F., Ikebuchi, E., Kameda, H., et al., 2018. Computer-assisted cognitive remediation therapy increases hippocampal volume in patients with schizophrenia: a randomized controlled trial. BMC Psychiatry 18, 83.
Nazeri, A., Chakravarty, M.M., Rotenberg, D.J., Rajji, T.K., Rathi, Y., Michailovich, O.V., et al., 2015a. Functional consequences of neurite orientation dispersion and density in humans across the adult lifespan. J. Neurosci. 35, 1753–1762.
Nazeri, A., Chakravarty, M.M., Rotenberg, D.J., Rajji, T.K., Rathi, Y., Michailovich, O.V., et al., 2015b. Functional consequences of neurite orientation dispersion and density in humans across the adult lifespan. J. Neurosci. 35, 1753–1762.
Robinson, R.G., 1998. Relationship of depression to cognitive impairment. The Clinical Neuropsychiatry of Stroke: Cognitive, Behavioral and Emotional Disorders Following Vascular Brain Injury. Cambridge University Press, Cambridge.
Robinson, R.G., Jorge, R.E., 2016. Post-Stroke Depression: a Review. Am. J. Psychiatry 173, 221–231.
Robinson, R.G., Kubos, K.L., Starr, L.B., Rao, K., Price, T.R., 1984. Mood disorders in stroke patients. Importance of location of lesion. Brain 107, 81–93.
Smith, S., Jenkinson, M., Johansen-Berg, H., Rueckert, D., Nichols, T.E., Mackay, C.E., et al., 2006. Tract-based spatial statistics: voxelwise analysis of multisubject diffusion data. Neuroimage 31, 1487–1505.
Song, Y.K., Li, X.B., Huang, X.L., Zhao, J., Zhou, X.X., Wang, Y.L., et al., 2008. A study of neurite orientation dispersion and density imaging in wilson's disease. J. Magn. Reson. Imaging 48, 423–430.
Song, Y.K., Li, X.B., Huang, X.L., Zhao, J., Zhou, X.X., Wang, Y.L., 2018. A study of neurite orientation dispersion and density imaging in wilson's disease. J. Magn. Reson. Imaging 48, 423–430.
Starkstein, S.E., Robinson, R.G., Price, T.R., 1987. Comparison of cortical and subcortical lesions in the production of poststroke mood disorders. Brain 110, 1045–1059.
Winston, G.P., Micallef, C., Symms, M.R., Alexander, D.C., Duncan, J.S., Zhang, H., 2014. Advanced diffusion imaging sequences could aid assessing patients with focal cortical dysplasia and epilepsy. Epilepsy Res. 108, 336–339.
Wright, P., Albarracin, D., Brown, R.D., Li, H., He, G., Liu, Y., 2008. Dissociated responses in the amygdala and orbitofrontal cortex to bottom-up and top-down components of emotional evaluation. Neuroimage 39, 894–902.
Yasuno, F., Taguchi, A., Yamamoto, A., Kajimoto, K., Kazui, H., Sekiyama, A., et al., 2014. Microstructural abnormalities in white matter and their effect on depressive symptoms after stroke. Psychiatry Res. Neuroimage 223, 9–14.
Yesavage, J.A., Brink, T.L., Rose, T.L., Lum, O., Huang, V., Adey, M., et al., 1982. Development and validation of a geriatric depression screening scale: a preliminary report. J. Psychiatr. Res. 17, 37–49.
Zhang, H., Schneider, T., Wheeler-Kingshott, C.A., Alexander, D.C., 2012. NODDI: practical in vivo neurite orientation dispersion and density imaging of the human brain. Neuroimage 61, 1000–1016.
Zhang, J., Gregory, S., Scahill, R.I., Durr, A., Thomas, D.L., Lehericy, S., et al., 2018. In vivo characterization of white matter pathology in premanifest huntington's disease. Ann. Neurol. 84, 497–504.